# Unexpected tautomeric equilibria of the carbanion-enamine intermediate in pyruvate oxidase highlight unrecognized chemical versatility of thiamin

Danilo Meyer[a,1], Piotr Neumann[b,1], Eline Koers[a], Hanno Sjuts[a], Stefan Lüdtke[a], George M. Sheldrick[c], Ralf Ficner[b], and Kai Tittmann[a,2]

[a]Albrecht-von-Haller Institute and Göttingen Center for Molecular Biosciences, D-37077 Göttingen, Germany; [b]Institute for Microbiology and Genetics D-37077 Göttingen, Germany; and [c]Institute of Inorganic Chemistry, Georg-August University Göttingen, D-37077 Göttingen, Germany

Edited by Gregory A. Petsko, Brandeis University, Waltham, MA, and approved May 28, 2012 (received for review January 24, 2012)

**Thiamin diphosphate, the vitamin B1 coenzyme, plays critical roles in fundamental metabolic pathways that require acyl carbanion equivalents. Studies on chemical models and enzymes had suggested that these carbanions are resonance-stabilized as enamines. A crystal structure of this intermediate in pyruvate oxidase at 1.1 Å resolution now challenges this paradigm by revealing that the enamine does not accumulate. Instead, the intermediate samples between the ketone and the carbanion both interlocked in a tautomeric equilibrium. Formation of the keto tautomer is associated with a loss of aromaticity of the cofactor. The alternate confinement of electrons to neighboring atoms rather than $\pi$-conjugation seems to be of importance for the enzyme-catalyzed, redox-coupled acyl transfer to phosphate, which requires a dramatic inversion of polarity of the reacting substrate carbon in two subsequent catalytic steps. The ability to oscillate between a nucleophilic (carbanion) and an electrophilic (ketone) substrate center highlights a hitherto unrecognized versatility of the thiamin cofactor. It remains to be studied whether formation of the keto tautomer is a general feature of all thiamin enzymes, as it could provide for stable storage of the carbanion state, or whether this feature represents a specific trait of thiamin oxidases. In addition, the protonation state of the two-electron reduced flavin cofactor can be fully assigned, demonstrating the power of high-resolution cryocrystallography for elucidation of enzymatic mechanisms.**

crystallography | tautomerization | enzyme mechanism

Thiamin diphosphate (ThDP, **1**, Fig. 1*A*), the biologically active derivative of vitamin B1, is a bioorganic cofactor involved in many central biochemical reactions that generate acyl carbanion equivalents (1). The ThDP cofactor consists of a thiazolium ring where the conjugate base at carbon 2 (C2) acts as the primary reaction site, an aminopyrimidine that serves as an intramolecular Brønsted acid/base, and a diphosphate that anchors the cofactor to its associated protein via a divalent metal ion.

Consistent with Breslow's seminal studies on thiazolium models (2), the catalytic sequence of every ThDP enzyme commences with addition of the C2 carbanion to a substrate carbonyl, yielding a covalent substrate-cofactor conjugate (**2**, Fig. 1*A*). This step is followed by C—C bond cleavage (decarboxylation in case of α-keto acid substrates) that produces a C2α-carbanion (**3a**), and subsequent enzyme-controlled routes (3, 4). The carbanion is potentially stabilized with the enamine contributor (**3b**) through delocalization into the thiazolium ring. It has been widely assumed that this delocalization is a necessary component of the reaction pathway. In fact, crystallographic analysis suggested the presence of an accumulation of resonance-stabilized, enamine-type intermediates in some, but not all, ThDP enzymes; however, the structural resolution (1.8–2.5 Å) precluded an unambiguous assignment in all these instances (5–9).

Although formation of a resonance-stabilized enamine seems to be logical from an organochemical point of view, its potential stabilization as an enzymic intermediate raises a problem, because all reactions in ThDP enzymes that follow enamine formation require the reactivity at C2α to be that of a localized carbanion. Relaxation of the initial carbanion to the enamine form would release energy, and reaction via the carbanion would require energy to be added, decreasing the efficiency (throughput) of the reaction. Besides the enamine, a reactant-state overstabilization may potentially also occur at the stage of the free radical ThDP intermediate, which is formed upon one-electron oxidation of the carbanion-enamine and can be stabilized as a conjugated $\pi$-type radical. This "stability problem" is most relevant for the ThDP oxidase family, including pyruvate oxidase (POX), since both the carbanion-enamine and the free radical are on the pathway (6). POX contains FAD as an additional cofactor, which oxidizes the carbanion-enamine in the course of the redox-coupled acyl transfer to the acceptor phosphate, yielding acetyl phosphate as product. Our studies indicated a complex chemical coupling between electron and acyl transfer (*SI Appendix*, Fig. S1), according to which FAD becomes one-electron reduced by the carbanion-enamine first, before the substrate phosphate covalently adds to the thiamin radical formed in the process. This step is followed by second electron transfer from the phospho-ThDP radical to the FAD semiquinone (6, 10). Such coupling is demanding as it initially requires carbanion chemistry at C2α to promote one-electron reduction of FAD, while the local charge at C2α of the thereby formed ThDP radical must be immediately lowered to allow the negatively charged phosphate anion to attack. In a sense, the polarity of C2α has to be inverted from negative (carbanion-enamine, nucleophilic center) to more positive (radical, electrophilic center). If POX was to stabilize perfectly conjugated enamine and $\pi$-type radical intermediates, this would seemingly lead to an increase of the activation barriers for FAD reduction and nucleophilic attack of phosphate onto the ThDP radical. It is interesting to note in that context that the X-ray structure of the related ThDP radical in the ThDP enzyme pyruvate:ferredoxin oxidoreductase (PFOR) was not compatible with a planar ThDP radical (11), although EPR analysis suggested formation of a delocalized, $\pi$-type radical (12).

A hallmark of enzymic ThDP catalysis is the co-catalytic function of the aminopyrimidine, which, by virtue of the canonical *V*-conformation of ThDP in enzymes and the resultant proximity

Author contributions: K.T. designed research; D.M., P.N., E.K., H.S., S.L., and K.T. performed research; G.M.S. provided a pre-release version of crystallographic software Shelx-2011; D.M., P.N., G.M.S., R.F., and K.T. analyzed data; and K.T. wrote the paper.

The authors declare no conflict of interest.

This article is a PNAS Direct Submission.

Data deposition: The atomic coordinates and structure factors have been deposited in the Protein Data Bank, www.pdb.org (PDB ID codes 4FEG and 4FEE).

[1]D.M. and P.N. contributed equally to this study.

[2]To whom correspondence should be addressed. E-mail: ktittma@gwdg.de.

This article contains supporting information online at www.pnas.org/lookup/suppl/doi:10.1073/pnas.1201280109/-/DCSupplemental.

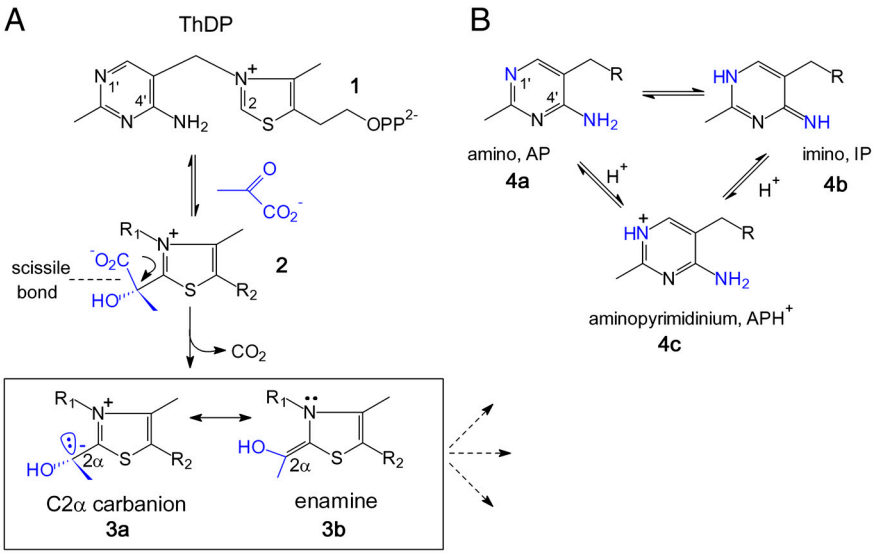


**Fig. 1.** Chemical structure of coenzyme ThDP and of key intermediates involved in the ThDP-catalyzed decarboxylation of α-keto acid pyruvate showing the thiazolium portion (*A*) and the different tautomers and ionization states of the co-catalytic aminopyrimidine (*B*). The carbanion-enamine intermediate, which is structurally described in this study, is boxed in (*A*).

of the 4′-amino group and the thiazolium C2, acts as a Brønsted acid/base catalyst in different stages of the reaction (13–16). Recently, spectroscopic evidence has been presented suggesting that the aminopyrimidine interconverts between the 4′-amino (AP, **4a**) and the 1′,4′-imino tautomer (IP, **4b**) with the positively charged, N1′-protonated aminopyrimidinium ($APH^+$, **4c**) as a presumed intermediate (Fig. 1*B*) (15, 16). It was shown for different enzymes that bond cleavage in the tetrahedral substrate-ThDP adducts and concomitant formation of the carbanion-enamine results in a change of the protonation state of the aminopyrimidine going from IP (substrate-ThDP) to $APH^+$/AP (carbanion-enamine). This finding pinpoints an intimate coupling between the thiazolium and aminopyrimidine in the course of substrate cleavage and carbanion-enamine formation that has yet to be fully explicated.

We have now determined the precise structure of the carbanion-enamine intermediate in POX from *Lactobacillus plantarum*. This enzyme is ideally suited to trap the pyruvate-derived hydroxyethyl-ThDP carbanion-enamine as a single, discrete intermediate to full occupancy (>95%) (17) (*SI Methods*). While our previous structural analysis of that intermediate was limited to a resolution of 2.29 Å (6), we succeeded in trapping this state at the level of true atomic resolution. The structure of this intermediate on the enzyme expands and in part revises our current understanding of enzymic ThDP catalysis as it suggests the existence of a tautomeric equilibrium of the carbanion with its ketone, whereas the expected enamine contributor is not accumulated.

## Results and Discussion

We determined two crystal structures of POX in complex with the ThDP carbanion-enamine and two-electron reduced FAD from two individual crystals at a resolution of 1.1 Å in each case (*SI Appendix*, Table S1). Both structures are identical but provide complementary information about hydrogen positions at the flavin and thiamin cofactors.

The structure of the hydroxyethyl-ThDP carbanion-enamine is very well defined in both active sites of the dimer in the asymmetric unit (Fig. 2*A* and *SI Appendix*, Figs. S2 and S3). The electron density is at the atomic centers of the intermediate atoms, suggesting that one discrete form of the carbanion-enamine has accumulated. However, as electron density is a space average over millions of unit cells, it could in principle originate from several carbanion-enamine forms with only subtle differences in their atomic positions that are not larger than their corresponding amplitude of thermal vibrations.

**Structure of the Thiazolium Heterocycle.** A very surprising and unexpected feature of the thiazolium is its marked out-of-plane distortion at ring carbon C2, which amounts to $0.26 \pm 0.02$ Å relative to the plane formed by the other ring atoms (Fig. 2*B*) [estimated standard deviation (esd) estimated by full-matrix refinement using Shelx-2011; bond-length esd's for thiamin and FAD vary between 0.01 and 0.02 Å]. This indicates a tetrahedral arrangement of the bonding around C2, which necessitates a loss of aromaticity of the thiazolium. In support of this model is the observed trigonal pyramidal geometry of N3, as well as an interatomic distance of $1.46 \pm 0.02$ Å between C2 and N3, which is indicative of single bond character (Fig. 2*B*). Conversely, a fully aromatic thiazolium as observed in small molecule crystal structures of thiamin models would require trigonal planar, $sp^2$-hybridized C2 and N3, and a C2—N3 double bond (1.31 Å) (*SI Appendix*, Fig. S4). The C2α atom of the intermediate in POX (derived from the carbonyl of pyruvate) is bound above the thiazolium ring. It, too, exhibits tetrahedral coordination, and the C2 and C2α interatomic distance of $1.49 \pm 0.02$ Å implies mainly single bond character (Fig. 2 *A* and *B*). The observation of apparent $sp^3$-hybridization states for both C2 and C2α cannot be explained by a single intermediate form of the carbanion-enamine even when all possible contributors, ionization states and tautomers are considered, as there is no imaginable species with $sp^3$-hybridized C2 and C2α (Fig. 3). That said, we can definitely exclude accumulation of the expected enol-enamine (**3b**) as it would require trigonal planar, $sp^2$-hybridized arrangements about both atoms in the C—C double bond (expected bond length 1.33 Å, experimentally determined bond length $1.49 \pm 0.02$ Å) (*SI Appendix*, Fig. S5). Formation of a distorted enamine, that is a pyramidalized alkene, is in our opinion an unlikely scenario, because a severe deviation from co-planarity of substituent arrangement is only reported for C—C double bonds located at the bridgehead positions of polycyclic structures (18). The tetrahedral coordination of C2 (Fig. 2*B*) rather suggests partial accumulation of a nonaromatic thiazolium with a pyramidal C2 carbanion (**3d**) and/or the C2-protonated form (**3e**), i.e., the enolate-carbanion (**3d**) or the thiazoline (**3e**) (Fig. 3), respectively, as previously demonstrated for thiazolium models (19). The detected out-of-plane distortion at C2 of the intermediate suggests

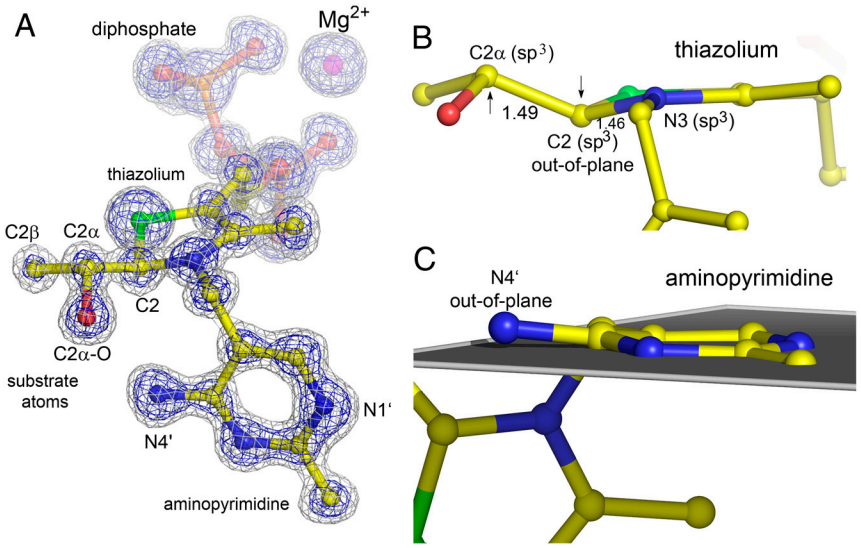


**Fig. 2.** Structure of the hydroxyethyl-ThDP carbanion-enamine intermediate trapped in pyruvate oxidase at a resolution of 1.1 Å. (*A*) The final refined model of the intermediate in ball-and-stick representation and the $Mg^{2+}$ ion as sphere are shown with the corresponding 2mFo-DFc electron density map contoured at different levels (blue: 4$\sigma$, grey: 2$\sigma$). (*B*) Side view of the carbanion-enamine highlighting the out-of-plane distortion at atoms C2 and C2α, and the apparent $sp^3$-hybridization states of atoms C2α, C2, and N3, which indicate a loss of aromaticity of the thiazolium heterocycle. The C2—N3 and C2—C2$\alpha$ bond lengths are indicated. (*C*) Side view of the aminopyrimidine highlighting the out-of-plane distortion at atom N4′ relative to the ring plane formed by the other atoms of the heterocycle. The structure of the carbanion-enamine is exemplified for active site A of crystal B, and all bond lengths of the C2-substituted thiazolium are shown in *SI Appendix*, Fig. S3 for both crystals.

that POX preferentially stabilizes the 3*S*-stereoisomer of the ketone (atom N3 is a lone-pair stereocenter) (*SI Appendix*, Fig. S6). In theory, the observed distorted intermediate may have been formed during data acquisition through reduction of the native enamine **3b** (photo-reduction of the C2—C2$\alpha$ double bond). We believe that this scenario is unlikely because we cannot detect any other chemical modification of amino acids or the flavin cofactor within the whole unit cell in all crystals tested. Second, structural characterization of the corresponding carbanion-enamine intermediate in transketolase highlighted a planar structure, although data acquisition was also carried out at a high-energy synchrotron (5).

Formation of nonaromatic thiazolium species, such as those suggested by the structure, would require deprotonation of C2$\alpha$—OH of the enol-enamine (**3b**) to give an enolate monoanion (**3c**/**3d**) (Fig. 3). Accumulation of a planar, resonance-stabilized enolate-enamine (**3c**) can be excluded based on the same premises as described above for the enol-enamine (**3b**). However, the mesomeric ketone-carbanion form of the enolate (**3d**) would be compatible with the observed $sp^3$-hybridization state of C2. The N4′ of the neighboring aminopyrimidine, stabilized as the 1′,4′-imino tautomer (IP, **4b**) in the pre-decarboxylation state (see below), is in close proximity (2.7 Å) to C2$\alpha$—O (Fig. 2*A*). It is not unreasonable to suggest that the imino-N4′ acts as a Brønsted base that deprotonates C2$\alpha$—OH. The thereby formed $APH^+$ cation (**4c**) could, in turn, protonate the C2 carbanion (**3d**) to give the C2-protonated thiazoline (**3e**), as the two atoms are located in close proximity (N4′-C2 distance 3.13 Å) (Figs. 2*A* and 3). Structural analysis indicates (*SI Appendix*, Fig. S7) that a favorable, i.e., almost perfectly linear proton transfer geometry is possible between C2$\alpha$—O and N4′ (angle C2$\alpha$—O—H—N4′ = 179.7°, optimal angle 180°). In contrast, potential proton transfer between N4′ and C2 is enthalpically unfavorable as it would have nonlinear geometry (N4′—H—C2 = 135.2°, deviation of approximately −45° from linearity).

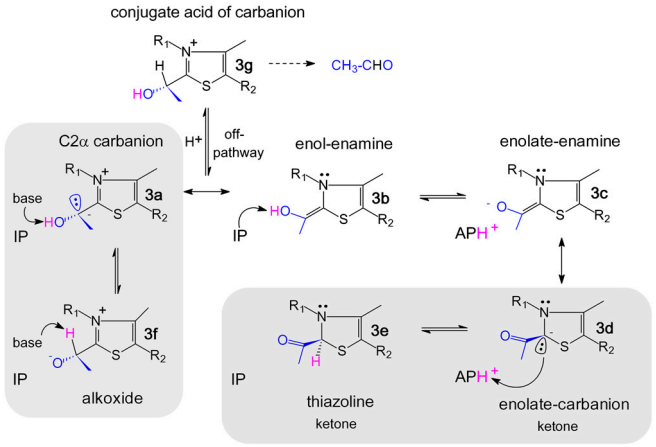


**Fig. 3.** Chemical structures of the hydroxyethyl-ThDP carbanion-enamine including possible tautomeric and ionization states. The expected corresponding state of the cofactor aminopyrimidine (IP, $APH^+$) is indicated. The substrate atoms are highlighted in blue, the dynamic hydrogen in magenta. Species suggested to be accumulated on POX are boxed.

The proposed internal proton transfer between C2$\alpha$—O and N4′ is supported by several independent lines of evidence. First, near-UV CD spectroscopic analysis of POX at different catalytic states demonstrates that the ThDP aminopyrimidine is predominantly stabilized as the 1′,4′-imino tautomer (IP, **4b**) bearing one hydrogen at N4′ at the pre-decarboxylation state (*SI Appendix*, Fig. S8). Subsequent formation of the carbanion-enamine goes along with an increase of $APH^+$ (**4c**) at the expense of IP (**4b**), such that N4′ is then in linkage with two hydrogen atoms. In support of the CD data is our observation of two positive difference electron density peaks close to N4′, the positions and intensities of which would be compatible with hydrogens in linkage to N4′ (*SI Appendix*, Fig. S9 *A*). In one active site of crystal A, the positions of all hydrogens at the aminopyrimidine can be assigned with confidence, supporting the proposed formation of $APH^+$ (*SI Appendix*, Fig. S10). Also, analysis of the anisotropic displacement parameters of the intermediate atoms reveals that the principal axis for displacement of atom N4′ is pointing towards C2$\alpha$—O along the potential proton transfer pathway (*SI Appendix*, Fig. S9 *B*). Such a feature would also be compatible with reversible interconversion between IP (**4b**) and $APH^+$ (**4c**) states driven by internal proton transfer between N4′ and C2$\alpha$—O.

If the nonaromatic keto tautomer of the carbanion-enamine with a $sp^3$-hybridized C2 (**3d** and/or **3e**) was to be the only intermediate species in pyruvate oxidase, C2α of the ketone functionality should be $sp^2$-hybridized and have a planar trigonal geometry (Fig. 3 and *SI Appendix*, Fig. S6). This is not supported by our experimental observation, which rather indicates an apparent tetrahedral nature of C2α (Fig. 2*B*). Hence, the ketone-carbanion (**3d**) or ketone-thiazoline (**3e**) must be in equilibrium with another intermediate form, in which the bonding around C2α is tetrahedral (electron density is a weighted average of both forms). There are three imaginable species with $sp^3$-hybridized C2α: *i*) the C2α-localized carbanion (**3a**), *ii*) the conjugate alkoxide tautomer (**3f**), and *iii*) the conjugate acid of the C2α-carbanion (**3g**) (Fig. 3). The latter would be an off-pathway intermediate driving the reaction towards formation of the nonphysiological product acetaldehyde, a reaction that is typically catalyzed by ThDP decarboxylases. How to discriminate between the three different species? First, we considered the possibility that the carbanion becomes protonated under equilibrium conditions yielding the conjugate acid of the carbanion (**3g**). We generated this intermediate on the enzyme using artificial substrate acetaldehyde (**3g** will be formed upon covalent addition of acetaldehyde to ThDP and must be deprotonated at C2α prior to redox reaction with FAD, *SI Appendix*, Scheme S1), and tested its kinetic competence. Our kinetic analysis revealed that **3g** is deprotonated to give **3a** with a first-order rate constant of 10.8± 1.4 $s^{-1}$ (*SI Appendix*, Fig. S11). In striking contrast, the "authentic" carbanion-enamine species that is accumulated after turnover of native substrate pyruvate is depleted with a $k_{obs} = 83.0\pm 0.5$ $s^{-1}$ when the enzyme returns to steady state turnover conditions (*SI Appendix*, Fig. S12). This finding relegates accumulation of **3g** to minor probability as it is not kinetically competent.

Therefore, the C2α carbanion (**3a**) and its conjugate alkoxide (**3f**) remain as possible alternatives. Although a localized carbanion would certainly be chemically and kinetically competent, one must critically ask whether a "naked" carbanion without any potential stabilization as e.g. delocalization would accumulate at equilibrium at the given pH 5.9. There are also problems associated with a potential formation of the conjugate alkoxide, as a concerted 1,2-migration of the proton from C2$\alpha$—O to C2α is unlikely due to very poor frontier orbital overlap. In addition, in POX, the substrate phosphate will directly attack C2α in a subsequent catalytic step (after 1$e^-$-oxidation of the carbanion-enamine by FAD). Consequently, any species with protonated C2α would not be chemically competent. To resolve this conundrum, we analyzed the interactions of the carbanion-enamine at the active site. Most intriguingly, we observe well-defined electron density for substrate phosphate atop the pyruvate-derived atoms of the intermediate (Fig. 4*A*). Phosphate is coordinated by multiple interactions with the main chain (Gly35, Ser36), several side chains (Ser36, Ser82, Gln122), and solvent molecules (W1, W2). Phosphate is further engaged in H-bonding interactions with both 2$\alpha$—O and C2α of the carbanion-enamine to give a ring-cyclic structure that could potentially comprise solvent molecule W1 (Fig. 4*A*). It is conceivable that such a cyclic structure could at least partially delocalize the negative charge over several atoms by rapid interconversion between the C2α carbanion (**3a**) (presumed interactions: C2$\alpha^-\cdots$**H**O-P; C2$\alpha$-O**H**$\cdots{}^-$O-P) and the conjugate alkoxide (**3f**) (presumed interactions: C2$\alpha$**H**$\cdots{}^-$O-P; C2$\alpha$-O$^-\cdots$**H**O-P) (Fig. 4*B*). Such carbanion-alkoxide "hybrid" would also provide needed stabilization of the carbanion by charge delocalization, yet would keep it kinetically accessible in rapid equilibrium.

Taken together, our analysis of the electron density maps suggest the carbanion-enamine to sample between two major states by internal proton transfer (Fig. 4*B*). In fact, we are able to fit the data with a model that includes both an aromatic tetrahedral form (**3a**/**3f**, fitted occupancy approximately 70%) as well as a nonaromatic ketone (**3d**/**3e**, fitted occupancy approximately 30%) (*SI Appendix*, Fig. S13). Further support for the proposed space average of a hydroxyethyl and a ketone species is provided by the refined atomic displacements parameters (*B*-factors), which are clearly higher for the substrate-derived atoms compared to those of the thiazolium and aminopyrimidine rings (*SI Appendix*, Fig. S14). Also, the calculated thermal ellipsoids of the intermediate atoms suggest the coexistence of (at least) two distinct chemical states rather than one discrete species (*SI Appendix*, Fig. S15).

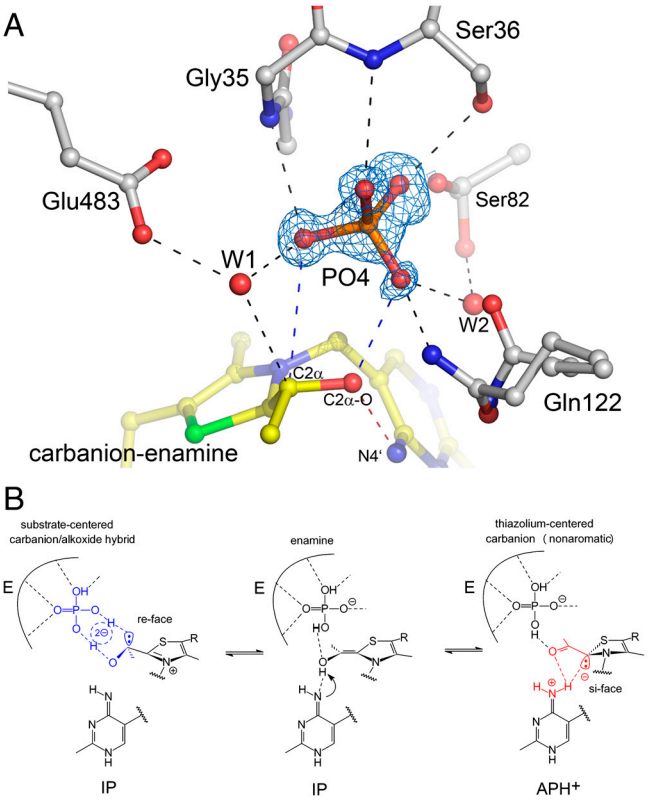


**Fig. 4.** Interactions of substrate phosphate with the carbanion-enamine and the protein. (*A*) Active site structure of POX showing the ThDP carbanion-enamine, selected amino acid residues, two solvent molecules, and electron density (blue, 2$\sigma$ contour level) assigned to originate from bound substrate phosphate. Hydrogen-bonding interactions of phosphate (<3.3 Å) are indicated. (*B*) Proposed structure of a ring-cyclic carbanion-alkoxide "hybrid" with delocalized negative charge that is in equilibrium with a nonaromatic thiazolium species.

**Structure of the Aminopyrimidine Heterocycle.** The aminopyrimidine of the intermediate also exhibits some unexpected structural features. The ring is slightly puckered, and most interestingly, atom N4′ of the 4′-amino group deviates by a few degrees from the plane formed by the other ring atoms (deviation of 10.02± 1.21°) (Fig. 2*C*). In crystal structures of thiamin models, atom N4' is coplanar with the pyrimidine ring atoms (maximal deviation of 1°). The observation of a strained aminopyrimidine in POX is counterintuitive, since a planar conformation with N4′ being in plane is expected for all of the different catalytically relevant forms (AP, IP, and APH$^+$, Fig. 1*B*). Strain is likely to be imposed by the protein, which forces ThDP to adopt the energy-rich *V*-conformation. Analysis of the interactions of the aminopyrimidine in the active site shows that N4′ forms an H-bond with the backbone carbonyl of Ala420 in addition to the aforementioned interaction with C2$\alpha$—O, while N1′ interacts with Glu59 (*SI Appendix*, Fig. S16). Noteworthy, these H-bonds do not exhibit perfect geometry (H-bond vectors are out-of-plane

with respect to aminopyrimidine). What could this high-energy conformation be good for? A possible hypothesis that remains to be tested is that the adopted conformation is required to allow for facile interconversion between the various protonic and tautomeric states of the aminopyrimidine as the intrinsically stored energy (strain) keeps the system reactive. Paraphrased, since all forms of the aminopyrimidine will be of high energy by virtue of the strained conformation, less energy is to be added to drive interconversion. Admittedly, a possible catalytic relevance of the out-of-plane distortion of N4′ is of speculative nature at this time and needs to be addressed in future studies. Another intriguing observation is the short interatomic distance between N1′ and Glu59 (2.61 Å), which falls below the critical distance of a low-barrier hydrogen bond (2.65 Å for O—N interactions) (20).

**Structure of the Two-Electron Reduced FAD.** Soaking of POX crystals with pyruvate eventually leads to complete consumption of physically dissolved substrate oxygen and two-electron reduction of the FAD cofactor. The electron density maps around FAD in one active site of crystal B are so well defined that the protonation state of the redox-active isoalloxazine can be assigned with confidence (Fig. 5*A*). While atom N5 is expectedly protonated as suggested by the pronounced positive difference electron density peak in its immediate vicinity, there is no such peak detectable close to N1 favoring accumulation of $FADH^-$ rather than of $FADH_2$ (Fig. 5*B*). The 2mFo-DFc electron density map suggests delocalization of the "second" electron involving N1 and neighboring atoms such as N10 rather than confining the second electron to N1. An intramolecular H-bond between a ribityl-OH (4—OH) and N1 is detected that could provide the means to destabilize a state with a protonated N1. Surprisingly, electron density originating from bound substrate pyruvate is observed close to N5 of $FADH^-$(*SI Appendix*, Fig. S17). The structure suggests an H-bonding interaction between N5—H and the carbonyl of pyruvate. This interaction is unlikely to persist after reoxidation of the flavin by oxygen because N5 would then become an H-bond acceptor. Hence, it seems that pyruvate is kept in place as long as the flavin is reduced and only becomes freed to react with ThDP upon reoxidation of FAD. Such a "redox-sensing" docking site could prevent pyruvate from off-pathway electrophilic attack onto the ThDP carbanion-enamine that readily accumulates at limiting oxygen concentrations (*SI Appendix*, Fig. S18).

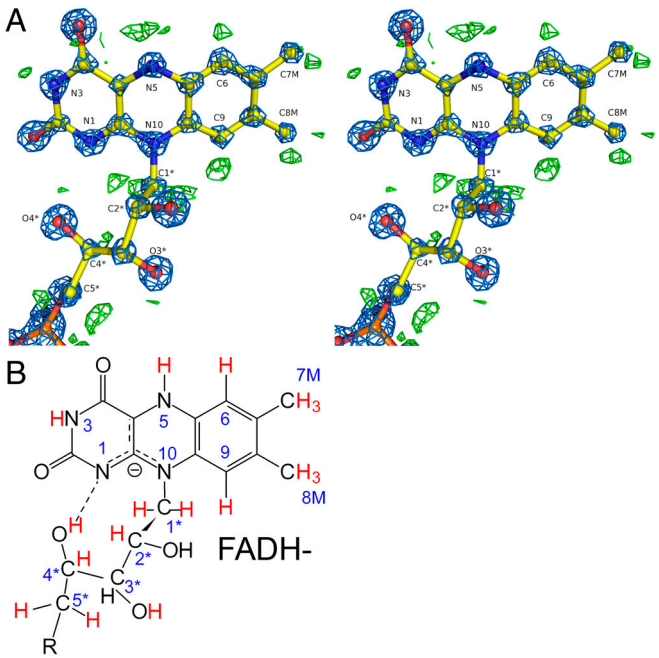


**Fig. 5.** Complete assignment of the protonation state of two-electron reduced FAD in POX. (*A*) Stereo view of the final refined model, the corresponding 2Fo-Fc electron density map (blue, contour level 5$\sigma$), and the $\sigma_A$-weighted Fo-Fc difference electron density map (green, contour level 3$\sigma$, carved 1.5 Å around FAD). Positive peaks in the difference density map are only observed for expected hydrogen "riding positions." Detected and assigned hydrogens are highlighted in red color in (*B*). Note that the electron density maps suggest accumulation of $FADH^-$ rather than $FADH_2$.

## Conclusions

Our structural studies on POX demonstrate that ThDP enzymes, classically assumed to stabilize carbanions by delocalization and formation of enamine contributors (1–4), have evolved alternative routes with intermediates that can promote progress to the products. Arguing against the accepted mechanism of ThDP action, the X-ray structural analysis of the carbanion-enamine excludes that the enamine has accumulated on POX. The electron density around the intermediate is not compatible with one discrete form of the carbanion-enamine but rather suggests an equilibrium between a substrate-centered hydroxyethyl carbanion-alkoxide "hybrid" (**3a⇔3f**) and a nonaromatic thiazolium species bearing a ketone functionality (**3d** and/or **3e**) (Fig. 4*B*). Tautomerization seems to be driven by internal proton transfer between the thiazolium-bound substrate moiety and the cofactor aminopyrimidine involving atom N4′.

We hypothesize that a tautomeric equilibrium (reversible ketonization) is of catalytic advantage for POX. In this enzyme, the carbanion-enamine undergoes $1e^-$-oxidation by FAD first, followed by nucleophilic attack of substrate phosphate onto the thereby formed ThDP radical (*SI Appendix*, Fig. S1). This sequence of elementary steps demands the polarity of the reacting substrate carbon C2α to be inverted from negative (nucleophilic center for FAD reduction) to positive (electrophilic center to allow attack of phosphate) (21). While the reducing power of a substrate-centered carbanion (**3a**) is qualified to promote FAD reduction, any keto form of the carbanion-enamine (**3d**/**e**) seems to have no obvious role for the initial redox reaction. However, if POX was to sample between hydroxyethyl and ketone species also after $1e^-$ oxidation of the carbanion-enamine by FAD, one of the formed ThDP radical species would be a ketone-type acetyl radical, of which the reacting C2α carbon is fairly electrophilic to allow attack by phosphate (*SI Appendix*, Fig. S19). Such a ketone radical would seem more reactive towards phosphate than a resonance-stabilized $\pi$-type radical. It hence appears that the observed ketonization of the carbanion-enamine foreshadows a similar scenario for the free ThDP radical, where substrate atom C2α must be an electrophilic center.

It is currently unclear why exactly the enamine does not accumulate on POX as it should be of lower energy compared to a carbanion. Most likely, productive interactions (binding energy) of the intermediate with the protein and substrate phosphate account for the needed stabilization of reactive carbanion states. The lone pair orbitals at C2α and C2 of the two interconverting carbanions are in antiperiplanar orientation (see Fig. 4*B*), and they appear to specifically interact with groups located at opposite chemical faces of the thiazolium. While the substrate moiety with atoms C2α and C2*α*—OH interacts with phosphate bound at the *re*-face of the thiazolium, involving a cyclic hydrogen-bonding network that delocalizes the charge at C2α (Fig. 4*B*), a potential C2-centered carbanion could be stabilized by a hydrogen-bond interaction with N4′ of the aminopyrimidine located at the *si*-face (or even proton transfer).

Finally, we wish to note that using the term "carbanion-enamine" as the common intermediate in ThDP catalysis is not sufficient to account for the dynamic equilibrium of the different possible contributors, tautomers, and ionization states as shown here for POX. Similar information will be required for other ThDP enzymes in order to correlate electronic and structural features of inter-

mediates with the specificity of the associated reaction. It will be interesting to learn whether the internal tautomerization is common to all ThDP enzymes or unique to ThDP oxidases. While oxidases require an interconversion between a nucleophilic and electrophilic substrate center, in most other ThDP enzymes a "pure" nucleophilic center needs to be established. However, a tautomerization would provide "stable storage" of the carbanion oxidation state, which is needed for further reaction.

Our study also demonstrates the power of high-resolution X-ray crystallography for detecting fine-structural details of reaction intermediates such as out-of-plane distortions, and for assigning protonation states of cofactors and intermediates, features that cannot be detected at "normal" resolution. In our study, we were able to capture an "averaged snapshot" of an equilibrium between two intermediate forms, which differ only in the position of a single catalytic hydrogen, an observation with strong implications for the mechanism.

## Materials and Methods

Pyruvate oxidase from *Lactobacillus plantarum* was crystallized by the hanging-drop vapor-diffusion method as previously described (6). Prior to data collection, crystals were soaked with substrate pyruvate for 30–60 sec. Data were processed and scaled with XDS (22). Iterative cycles of model building and refinement were carried out using COOT, PHENIX, and SHELX software as detailed in *SI Appendix* (23–25).

**ACKNOWLEDGMENTS.** We gratefully acknowledge discussions with Ron Kluger, Sandro Ghisla, Richard Schowen, Michael McLeish, and Ralph Golbik and their insightful comments on the manuscript.

1. Schowen RL (1998) Thiamin-dependent enzymes. *Comprehensive Biological Catalysis*, ed ML Sinnott (Academic Press, London), Vol 2, pp 217–266.
2. Breslow R (1957) The mechanism of thiamine action. 2. Rapid deuterium exchange in thiazolium salts. *J Am Chem Soc* 79:1762–1763.
3. Kluger R, Tittmann K (2008) Thiamin diphosphate catalysis: Enzymic and nonenzymic covalent intermediates. *Chem Rev* 108:1797–1833.
4. Jordan F (2003) Current mechanistic understanding of thiamin diphosphate-dependent enzymatic reactions. *Nat Prod Rep* 20:184–201.
5. Fiedler E, et al. (2002) Snapshot of a key intermediate in enzymatic thiamin catalysis: Crystal structure of the alpha-carbanion of (alpha,beta-dihydroxyethyl)-thiamin diphosphate in the active site of transketolase from Saccharomyces cerevisiae. *Proc Natl Acad Sc USA* 99:591–595.
6. Wille G, et al. (2006) The catalytic cycle of a thiamin diphosphate enzyme examined by cryocrystallography. *Nat Chem Biol* 2:324–328.
7. Machius M, et al. (2006) A versatile conformational switch regulates reactivity in human branched-chain alpha-ketoacid dehydrogenase. *Structure* 14:287–298.
8. Berthold CL, et al. (2007) Crystallographic snapshots of oxalyl-CoA decarboxylase give insights into catalysis by nonoxidative ThDP-dependent decarboxylases. *Structure* 15:853–861.
9. Suzuki R, et al. (2010) Crystal structures of phosphoketolase: Thiamine diphosphate-dependent dehydration mechanism. *J Biol Chem* 285:34279–34287.
10. Tittmann K, et al. (2005) Radical phosphate transfer mechanism for the thiamin diphosphate- and FAD-dependent pyruvate oxidase from Lactobacillus plantarum. Kinetic coupling of intercofactor electron transfer with phosphate transfer to acetyl-thiamin diphosphate via a transient FAD semiquinone/hydroxyethyl-ThDP radical pair. *Biochemistry* 44:13291–13303.
11. Chabriere E, et al. (2001) Crystal structure of the free radical intermediate of pyruvate: Ferredoxin oxidoreductase. *Science* 294(5551):2559–2563.
12. Mansoorabadi SO, et al. (2006) EPR spectroscopic and computational characterization of the hydroxyethylidene-thiamine pyrophosphate radical intermediate of pyruvate: Ferredoxin oxidoreductase. *Biochemistry* 45:7122–7131.
13. Kern D, et al. (1997) How thiamine diphosphate is activated in enzymes. *Science* 275:67–70.
14. Schellenberger A (1998) Sixty years of thiamin diphosphate biochemistry. *Biochim Biophys Acta* 1385:177–186.
15. Nemeria N, et al. (2007) The 1′,4′-iminopyrimidine tautomer of thiamin diphosphate is poised for catalysis in asymmetric active centers on enzymes. *Proc Natl Acad Sci USA* 104:78–82.
16. Nemeria NS, Chakraborty S, Balakrishnan A, Jordan F (2009) Reaction mechanisms of thiamin diphosphate enzymes: Defining states of ionization and tautomerization of the cofactor at individual steps. *FEBS J* 276:2432–2446.
17. Tittmann K, et al. (2003) NMR analysis of covalent intermediates in thiamin diphosphate enzymes. *Biochemistry* 42:7885–7891.
18. Vazquez S, Camps P (2005) Chemistry of pyramidalized alkenes. *Tetrahedron* 61:5147–5208.
19. Chen YT, Barletta GL, Haghjoo K, Cheng JT, Jordan F (1994) Reactions of benzaldehyde with thiazolium salts in Me(2)So—Evidence for initial formation of 2-(alpha-hydroxybenzyl)thiazolium by nucleophilic-addition and for dramatic solvent effects on benzoin formation. *J Org Chem* 59:7714–7722.
20. Cleland WW, Frey PA, Gerlt JA (1998) The low barrier hydrogen bond in enzymatic catalysis. *J Biol Chem* 273:25529–25532.
21. Tittmann K (2009) Reaction mechanisms of thiamin diphosphate enzymes: Redox reactions. *FEBS J* 276:2454–2468.
22. Kabsch W (1993) Automatic processing of rotation diffraction data from crystals of initially unknown symmetry and cell constants. *J Appl Crystallogr* 26:795–800.
23. Emsley P, Cowtan K (2004) Coot: Model-building tools for molecular graphics. *Acta Crystallogr Sect D Biol Crystallogr* 60:2126–2132.
24. Adams PD, et al. (2002) PHENIX: Building new software for automated crystallographic structure determination. *Acta Crystallogr Sect D Biol Crystallogr* 58:1948–1954.
25. Sheldrick GM (2008) A short history of SHELX. *Acta Crystallogr Sect A* 64:112–122.